Estimation of Residual Flexural Capacity of Existing Precast Concrete Panels by Visual Inspection

J. Miljan[1] and M. Kiviste[2]

[1]Institute of Forestry and Rural Engineering, Estonian University of Life Sciences, Kreutzwaldi 5, 51014 Tartu, Estonia; e-mail: jaan.miljan@emu.ee
[2]Institute of Forestry and Rural Engineering, Estonian University of Life Sciences, Kreutzwaldi 5, 51014 Tartu, Estonia; e-mail: mihkel.kiviste@emu.ee

Abstract. The influence of visual assessment grade on the residual flexural capacity of 46 existing precast concrete ribbed panels was studied. Before the tests, the panels were assessed on a 6-point rating scale according to visually distinguishable corrosion deterioration. All panels, the ultimate load of which was lower than the control load, received grade 0 on visual rating scale. Consequently, attention should be paid to panels where the concrete cover of longitudinal reinforcement has spalled (grade 0), which could be a sign of decreasing load capacity. The majority of panels with grade 0 exhibited larger deflections under load than panels with higher grades. Of the 46 panels tested flexural ductile failure was noticed in 36 panels.

Key words: Visual grade, residual flexural capacity, corrosion, precast ribbed panels.

INTRODUCTION

In Estonia, the bearing structures of many existing agricultural and industrial buildings constitute a precast concrete skeletal frame. Particularly intensive construction based on industrially produced (precast) elements started in the 1960s when standardized design solutions and reinforced concrete structure designs were employed. However, the initial signs of corrosion of steel reinforcement became evident in agricultural buildings already in the 1970s. Corrosion was initiated by carbonation, because of high content of carbon dioxide and moisture in the air of an agricultural building. Aggressive indoor microclimate together with relatively porous concrete was the main reason for the high rate of carbonation. Department of Rural Building of Estonian University of Life Sciences (EMU) has gathered data describing the state of concrete load-bearing structures (columns, beams and ribbed panels) in 258 agricultural buildings from 1974 to 1997 assigning grades to 23,336 ribbed ceiling panels (i.e. about 3.5% of the total number of panels in agricultural buildings of Estonia) (Miljan R, 2005). The structures have been visually assessed, using a 6-point scale to reflect the externally distinguishable corrosion damage (Miljan J, 1977). According to this scale grade, 5 corresponds to no visual reinforcement corrosion deterioration detected, and grade 0 to concrete cover that has spalled.

There are about 4,000 agricultural buildings with an average floor space of 1,800m^2 in Estonia today. Many of their precast concrete load-bearing members

(columns, beams and ribbed panels) are in service with a cracked or spalled concrete cover. The owners of buildings are most likely concerned about the condition and residual strength of their concrete structures. There is an increasing demand for informed decisions about the capability of structure to serve its intended function or, otherwise, the need for repair or demolition.

This paper reports an experimental study of 14 precast non-prestressed concrete ribbed panels of mark PKZH-2 and 32 prestressed concrete panels of mark PNS-3, PNS-12, and PNS-14. Intentionally, panels in poor condition, i.e. with cracked (grade 1) or spalled concrete cover in longitudinal rib (grade 0) were chosen for structural tests to specify their residual ultimate strength and flexural behaviour. The marks of panels reflect the former Soviet standard GOST. Precast ribbed panels with aforementioned marks are common in the industrial and agricultural buildings of Estonia (but also in other former Soviet countries), built from 1950s to 1990s. All tested ribbed ceiling and roof-ceiling panels had a length of 5970mm and width of 1490mm (Fig. 1).

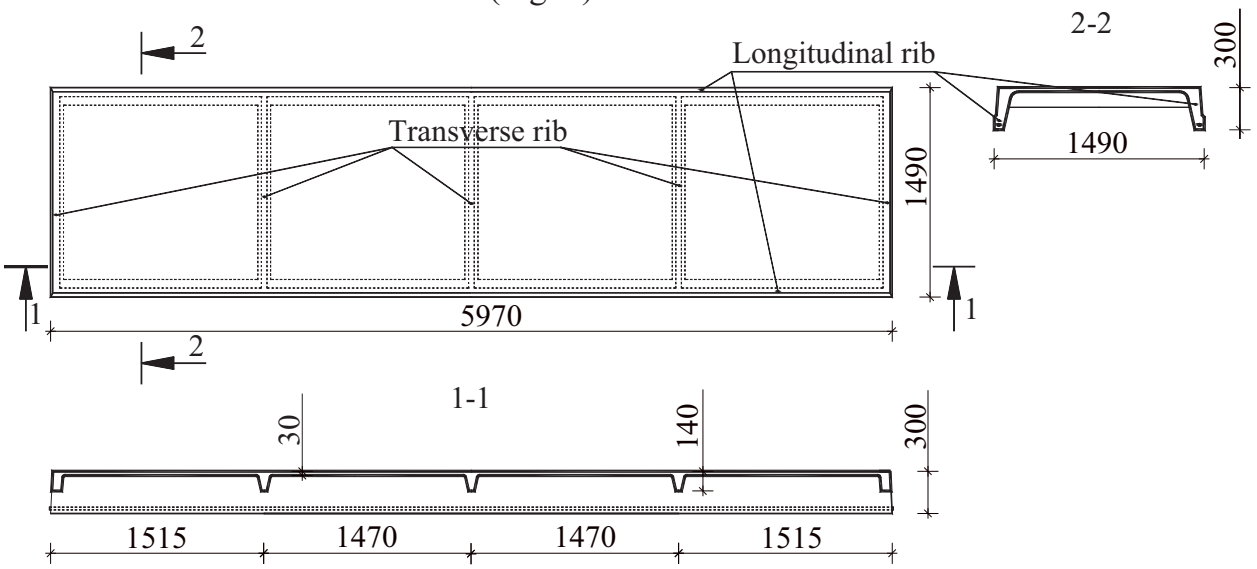

Fig. 1. Top view, longitudinal and transversal section of a precast ribbed panel

Non-prestressed concrete panels of mark PKZH were manufactured (in accordance with GOST 7740-55) from the 1950s until 1964…1965. Prestressed concrete panels of mark PNS were produced from 1964…1965 until at least 1990. Panels PNS-3 was produced in the relatively short period of transition from panel mark PKZH to PNS. Since the mid-1960-ies, production of panels PNS-12 (a further development of PNS-3) and PNS-14 started (Series PK-01-111, 1961).

Over the past few decades, research has been conducted to study the effect of corrosion on the mechanical behaviour of concrete beams or slabs by using accelerated corrosion tests in laboratory. However, laboratory studies cannot fully represent all the aspects of the on-site behaviour of concrete structures. Unfortunately, structural tests concerning the existing corroded reinforced concrete members (Durham et al., 2007; Heymsfield et al., 2007) are rare. Research objects are difficult to find since the owners wish to exploit the concrete structures of a building as long as possible and not to give them away for testing.

Consequently, the first objective of the research is to find the residual flexural strength and behaviour of the existing precast concrete ribbed panels. The second objective is to clarify whether it is possible to estimate the load capacity of a ribbed panel according to visually discernible corrosion damage. Methods that can correlate visual damage with rating categories that are indicative of structural performance are lacking (Higgins & Farrow, 2006).

Research significance. Numerous studies have been conducted regarding chloride or CO_2 penetration and prediction of corrosion initiation. However, few investigators have dealt with corrosion propagation and even fewer with residual load capacity of corroded concrete structures. Unfortunately, tests with real, existing structures are scarce in literature, but those are valuable to substantiate the findings from laboratory study with accelerated corrosion. This study presents the results of visual assessment and flexural tests of 46 existing precast concrete ribbed panels. The reported data are relevant as an experimental reference to models employed in a long service life, structural capacity predictions, and repair optimization.

MATERIALS AND METHODS

Visual scale for assessing the degree of deterioration. Before structural tests, the panels were assessed on a scale developed at the Chair of Structural Mechanics of the former Estonian Agricultural Academy (now EMU) in 1974. Grades were applied to assess visually the changes in the functional state of the panels based on the condition of steel reinforcement and concrete cover. The visual assessment scale distinguishes between six different states as shown in Table 1. If even one feature of a lower grade can be determined during the inspection process, this lower grade is assigned to the reinforced concrete ribbed panel.

Table 1. Classification of deterioration states of the ribbed ceiling panels

Grade	Description of state
5	No corrosion detected
4	1) Less than 20% of the concrete cover of a slab has spalled; 2) Noticeable longitudinal cracks (0.3-1.0mm) in transverse ribs.
3	1) More than 20% of the concrete cover of slab reinforcement has spalled; 2) Less than 20% of the concrete cover of stirrups in the longitudinal ribs has spalled; 3) In transverse ribs wide (>1.0mm) cracks have occurred; 4) Less than 20% of the concrete cover in transverse ribs has spalled.
2	1) More than 20% of the concrete cover of stirrups in longitudinal ribs has spalled; 2) More than 20% of the concrete cover of reinforcement in transverse ribs has spalled; 3) Longitudinal micro cracks (0-0.3mm) due to corrosion in longitudinal ribs.
1	Longitudinal cracks (> 0.3mm) in longitudinal ribs;
0	Concrete cover of the reinforcement in longitudinal ribs has spalled.

Changes in the condition of structures estimated by visual inspection are best described by the assessment of the different deterioration states of ribbed ceiling panels. Ribbed panels have different thickness of concrete cover and diameter of reinforcing bars in slabs, transversal and longitudinal ribs. For example, the ribbed panel of mark PNS-12 has a 10mm concrete cover in the slab, 15mm in transversal and 25mm in longitudinal rib (Series PK-01-111, 1961). This means that in the case of carbonation induced corrosion, generally, the first visual deterioration will first occur in slabs, then in transversal ribs and, finally, in longitudinal ribs.

Structural test series. In this research, structural tests with 46 existing reinforced and pre-stressed concrete ribbed panels were carried out to find their residual flexural capacity. Current study is based on the series of tests of ribbed panels at EMU since 1973. 14 reinforced concrete (RC) panels of mark PKZH-2 and 32 pre-stressed concrete (PC) panels of mark PNS-3, PNS-12 and PNS-14 were tested. Generally, the mark was painted on the panel after curing in the factory already. In the absence of the painted mark, the diameter of the longitudinal working rebar was measured to determine the mark of a panel. The length and width of all panels were 5970mm and 1490mm, respectively. The summary of test series is presented in Table 2. Letter(s) in the first column is associated with the location of panels. RC panels are marked with a hyphen between the letter and the number, while PC panels are marked without a hyphen.

Table 2. Test series of reinforced and prestressed concrete ribbed panels

Panels (amount)	Mark	Object and purpose	Test location	Loading, location	Test year	Age of panels	Test performer
K-1 ... K-7 (7)	PKZH-2	Kärstna pigsty	Kärstna field tests	Sand uniformly, soil	1973	12	J. Miljan
K-8 ... K-10 (3)	PKZH-2	Kärstna pigsty	Tallinn, test hall	Cast iron loads uniformly, RC floor	1974	13	J. Miljan
P11 ... P13 (3)	PNS-3	Pandivere pigsty	Tallinn, test hall	Cast iron loads uniformly, RC floor	1974	10	J. Miljan
VA14 … VA19 (6)	PNS-3	Vao pigsty	Vao field tests	RC foundation blocks uniformly, soil	1975	11	J. Miljan
T-20 … T-23 (4)	PKZH-2	Torma cowshed	Torma field tests	RC curbstones uniformly, soil	1978	15	J. Miljan
L1 … L10 (10)	PNS-12. PNS-14	Luha cowshed	Tartu, EMU lab	Hydrocylinder, 4-point bending, RC force floor	2000 - 2001	26	E. Laiakask
R1 … R8 (8)	PNS-12	Raadi garage	Tartu, EMU lab	Hydrocylinder, 4-point	2002	Un-know	M. Kiviste,

				bending, RC force floor		n	H. Tomann, M. Tarto
V8 … V12 (5)	PNS-12, PNS-14	Corridor of Vara pigsty	Tartu, EMÜ lab	Hydrocylinder, 4-point bending, RC force floor	2005	32	R. Halgma, L. Linnus, T. Salu

As shown in Table 2, all tested panels had been in service for at least 10 years. The panels were demounted and singly loaded. The panels were tested in laboratory (K-8 - K-10, P11 - P13, L1 - L10, R1 - R8, V8 - V12) as well as on site (K-1 - K-7, VA14 - VA19, T-20 … T-23). Structural tests with pre-stressed ribbed panels of mark PNS-12 and PNS-14 are discussed in more detail in another paper.

The panels were lifted to RC blocks, which acted as sub supports. Singly tested panels were simply supported on a steel pin and roller support. All tested panels were loaded in increments of 10% of the control load (q_c) which was kept constant for at least ten minutes on each stage (GOST 8829-85).

The control load was set to test new panels issued from the factory. A few randomly chosen new panels were tested in the factory to check their crack resistance, rigidity and load capacity up to one increment higher than the control load. Repetition tests were due if the ultimate load of a panel issued from the factory was less than the control load but not less than 85% of the control load. The panels did not meet the strength requirements, if a single ultimate load in primary or repetition tests would be less then 85% of the control load (Series PK-01-111, 1961). The design load (q_d) was implemented by the structural engineering design of a building.

In all test series, uniformly distributed loads were imitated to compare the results with the control and design load. The panels were tested to failure or limit state, where deflections of a panel increased without additional load (GOST 8829-85). The maximum load a panel could carry was recorded as the ultimate load (q_u). The existing cracks and cracks developing during the test were carefully recorded with a marker on the panel surface.

Vertical displacements were measured at four corners (on supports) and on both longitudinal ribs at the mid-span of a panel. Generally, precision dial gauges of 0.01mm were applied at the corners and compliant measuring gauges (type Maksimov) of precision 0.1mm and 0.01mm at mid-span of a rib. The mid-span deflection of a panel was calculated as a difference of the mean mid-span deflection of both longitudinal ribs and of the mean displacement at panel supports (GOST 8829-85).

RESULTS AND DISCUSSION

Ultimate residual strength of existing ribbed panels. To compare the residual strength of panels of 4 different marks, the ratio (q_u/q_c) of ultimate load and control load was calculated. The one-way analysis of variance (ANOVA) did not reveal significant difference in the average ratio of ultimate load and control load by the panel marks (PKZH-2, PNS-3, PNS-12, PNS-14) at the confidence level

$\alpha=0.05$. Also, for purpose of comparison, the ultimate load (q_u) of test panels was divided by the design load (q_d).

The control loads of panels PKZH-2, PNS-3 (later PNS-12) and PNS-14 are 387 (GOST 7740-55), 750 (Series PK-01-111, 1961) and 1440 kgf/m^2 (Series PK-01-111, 1961), transformed to kN/m^2 in Fig. 4-7, respectively. The design loads of panels PKZH-2, PNS-3 (later PNS-12) and PNS-14 are 270 (GOST 7740-55), 460 (Series PK-01-111, 1961) and 950 kgf/m^2 (Series PK-01-111, 1961), transformed to kN/m^2 in Fig. 4-7, respectively. The results of visual assessment and flexural test of ribbed panels are presented in Table 3.

Table 3. Results of visual assessment and flexural test of ribbed panels

Panel	Mark	Grade	q_u, kN/m^2	q_u/q_c	q_u/q_d	Failure mode
K-1	PKZH-2	0	4.52	1.19	1.71	TR
K-2	PKZH-2	1	5.18	1.36	1.96	FD
K-3	PKZH-2	0	3.97	1.05	1.50	FD
K-4	PKZH-2	1	4.79	1.26	1.81	FD
K-5	PKZH-2	1	5.16	1.36	1.95	FD
K-6	PKZH-2	0	4.31	1.14	1.63	LR
K-7	PKZH-2	1	4.54	1.20	1.71	TR
K-8	PKZH-2	0	4.10	1.08	1.55	FD
K-9	PKZH-2	0	2.67	0.70	1.01	FD
K-10	PKZH-2	0	2.67	0.70	1.01	SU
P11	PNS-3	2	11.01	1.50	2.44	FD
P12	PNS-3	1	8.07	1.10	1.79	FD
P13	PNS-3	2	9.56	1.30	2.12	FD
VA14	PNS-3	1	8.79	1.19	1.95	FD
VA15	PNS-3	1	8.79	1.19	1.95	FD
VA16	PNS-3	2	9.90	1.35	2.20	FD
VA17	PNS-3	2	9.90	1.35	2.20	FD
VA18	PNS-3	2	9.90	1.35	2.20	FD
VA19	PNS-3	2	9.90	1.35	2.20	FD
T-20	PKZ-2	1	5.64	1.49	2.13	FD
T-21	PKZ-2	2	5.94	1.57	2.24	FD
T-22	PKZ-2	1	5.64	1.49	2.13	FD
T-23	PKZ-2	1	5.43	1.43	2.05	FD
L1	PNS-12	0	9.00	1.23	2.00	FD
L2	PNS-12	4	9.20	1.25	2.04	FD
L3	PNS-12	1	9.25	1.26	2.05	FD
L4	PNS-12	3	9.70	1.30	2.15	FD
L5	PNS-12	1	9.75	1.33	2.16	FD
L9	PNS-12	3	9.04	1.23	2.00	FD
L6	PNS-14	5	16.95	1.20	1.82	FD
L7	PNS-14	0	13.56	0.96	1.46	WR
L8	PNS-14	0	10.17	0.72	1.09	WR
L10	PNS-14	0	15.82	1.12	1.70	SH
R1	PNS-12	0	8.35	1.14	1.85	FD
R2	PNS-12	0	7.26	0.99	1.61	FD

R3	PNS-12	1	9.12	1.24	2.02	FD
R4	PNS-12	1	9.64	1.31	2.14	FD
R5	PNS-12	1	9.86	1.34	2.19	FD
R6	PNS-12	0	8.59	1.17	1.90	FD
R7	PNS-12	1	7.91	1.08	1.75	WR
R8	PNS-12	0	8.28	1.13	1.84	FD
V8	PNS-12	0	9.00	1.22	2.00	SH
V9	PNS-12	0	10.53	1.43	2.33	FD
V10	PNS-12	1	8.80	1.20	1.95	FD
V11	PNS-12	2	9.30	1.26	2.06	FD
V12	PNS-14	1	15.28	1.08	1.64	SH

Failure: FD – flexural ductile, TR – rebar rupture in transversal rib, LR – rebar rupture in longitudinal rib, SU – failure of longitudinal rib near support, WR – weld rupture at support, SH – shear.

The influence of visual appearance (grade) on load capacity (q_u/q_c) of 46 singly tested panels is presented in Fig. 2. Box plot in Fig. 2 was generated with statistical software R. The box plot shows the distribution of the data points around the median (thick horizontal line in Fig. 2), indicating upper and lower quartiles (horizontal edges of the box) and minimum and maximum values (ends of vertical bar).

Fig. 2 shows non-linear decreasing trend of q_u/q_c ratio with decreasing grade of panel. Only a few samples of high grades exist in the current data set. Neither statistical nor substantial reasons exist to assume a trend in q_u/q_c ratio at grade 2 or higher. However, box plots from grade 2 to 0 demonstrate evident decrease of q_u/q_c ratio. The one-way ANOVA revealed a significant effect for grades, $F(5,40) = 5.35;\ p = 0.0007$. The magnitude of the grade to q_u/q_c ratio was computed as $R^2 = 0.40$. The Tukey HSD test for multiple comparison of means proved a significant difference in q_u/q_c ratio between grade 0 and higher grades.

The ultimate load of only five of the 46 singly tested panels was less than the control load. All of these five panels received grade 0 on a visual rating scale. Consequently, attention should be paid to panels where the concrete cover of longitudinal reinforcement has spalled (grade 0), which could be a sign of decreased load capacity. The visual scale proposed in the paper has the potential to serve as a rational tool for practitioners, operators and asset managers to make decisions about the optimal timing for repairs, strengthening, and/or rehabilitation of corrosion-affected concrete infrastructure. Scale-acquainted engineers can rate reinforced concrete structures relatively quickly and simply to fetch out ribbed ceiling panels (if any) of the spalled concrete cover. Later on the residual flexural capacity of panels with grade 0 needs a structural expert's judgment.

It is also worth mentioning that no panels with a corrosion-induced crack in longitudinal rib (grade 1) were dangerous from the aspect of ultimate residual load capacity.

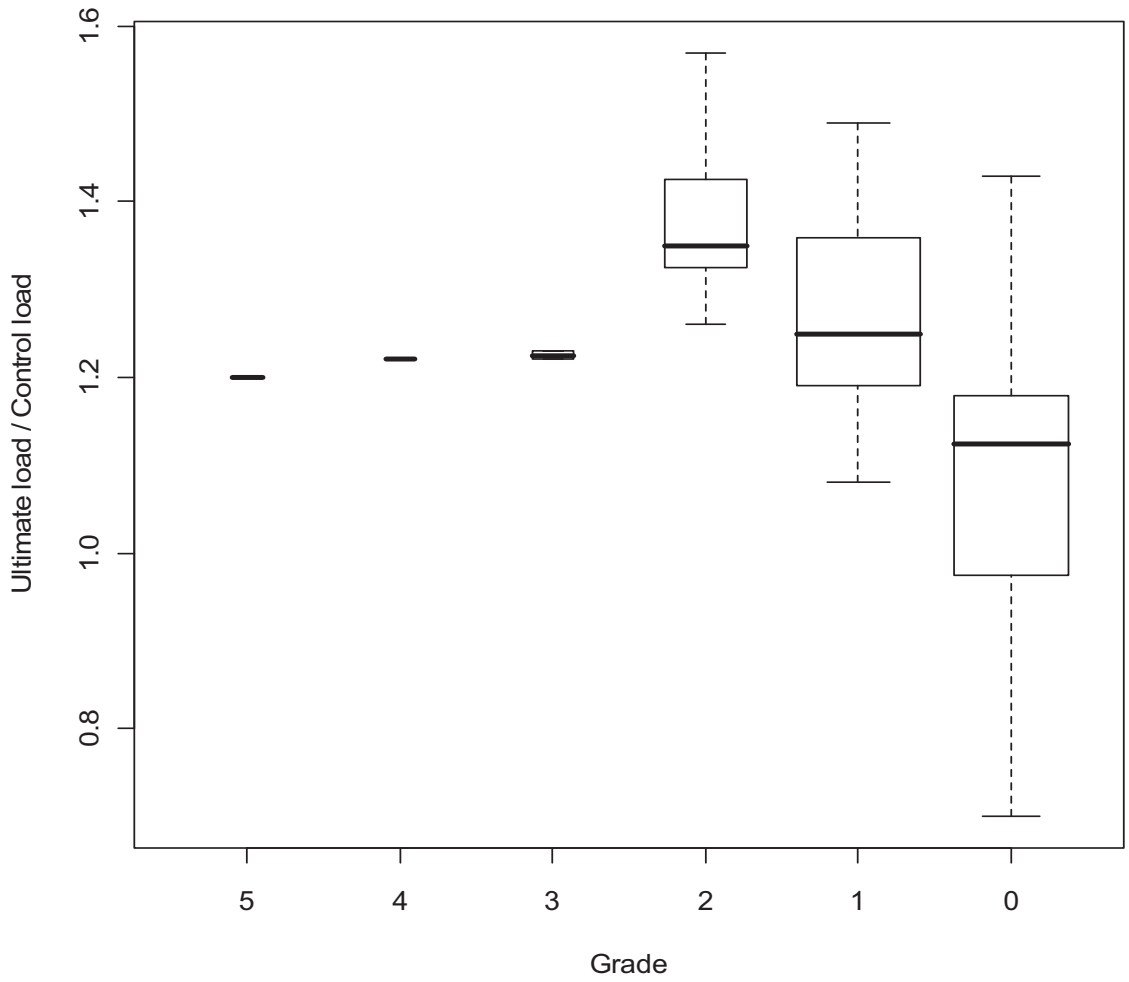

Fig. 2. Box plot of q_u/q_c ratio for singly tested panels of different visual grades. The box plots show distribution characteristics: the median (thick horizontal line), upper and lower quartiles (horizontal edges of the box) and minimum and maximum values (ends of vertical bar) of the q_u/q_c ratio by different grades

Fig. 2 demonstrates that q_u/q_c ratio varies the most in panels with a spalled concrete cover (grade 0). This means that panels, which may have just reached grade 0 as well as panels in critical state in terms of their load capacity are both rated as grade 0. Consequently, panels with a spalled concrete cover should be differentiated to specify their different residual load capacity. Deterioration states employed for panel classification in the current study (in Table 1) were developed already in 1974 and could be updated. Durham et al. (2007); Heymsfield et al. (2007) have tested 33 existing precast non-prestressed channel beams, which were used in short multi-span bridges in Arkansas in the 1950s through the early 1970s. The beams, constructed without shear reinforcement, were categorized as 'good', 'average' or 'poor' as a function of percentage and location of exposed longitudinal reinforcing steel. All these three classifications correspond to grade 0 on the visual rating scale of the current study.

The original objective of the study by Heymsfield et al. (2007) was to establish a correlation for inspection purposes between the beam's visual deteriorated state and its corresponding approximate structural capacity. 5.79m channel beams with similar cross section (ribbed slab) were tested also on a four-

point loading frame. It was found that the strength of beams was more a function of a concrete compressive strength rather than deterioration state.

Torres-Acosta et al. (2007) have proposed a durability model based on experimental load capacity values from various investigations (Tachibana et al., 1990; Almusallam et al., 1996; Almusallam et al., 1997; Huang & Yang, 1997; Rodriguez et al., 1997; Mangat & Elgarf, 1999), where results of different structural members (beams, slabs) under accelerated corrosion were presented. Unfortunately, the results of the current study are directly incomparable to the previously mentioned ones due to the absence of control data (new and not corroded) panels and rebar radius loss. Fig. 3 represents an illustrative load-capacity model for a reinforced (or pre-stressed) concrete flexural member (RCM) referred to in Torres-Acosta et al. (2007) and the current study with the addition of research results by Heymsfield et al. (2007) and Li et al. (2008). The model presents the structural load capacity of a RCM as a function of its lifetime. The lifetime T of the flexural member is defined as:

$$T = T_I + T_P + T_{RL} \tag{1}$$

where T_I is the corrosion initiation stage from the time of construction to the time of corrosion initiation; T_P is the corrosion propagation stage during which the steel corrodes until an unacceptable level of corrosion is reached; and T_{RL} is residual life stage from serviceability to ultimate limit state.

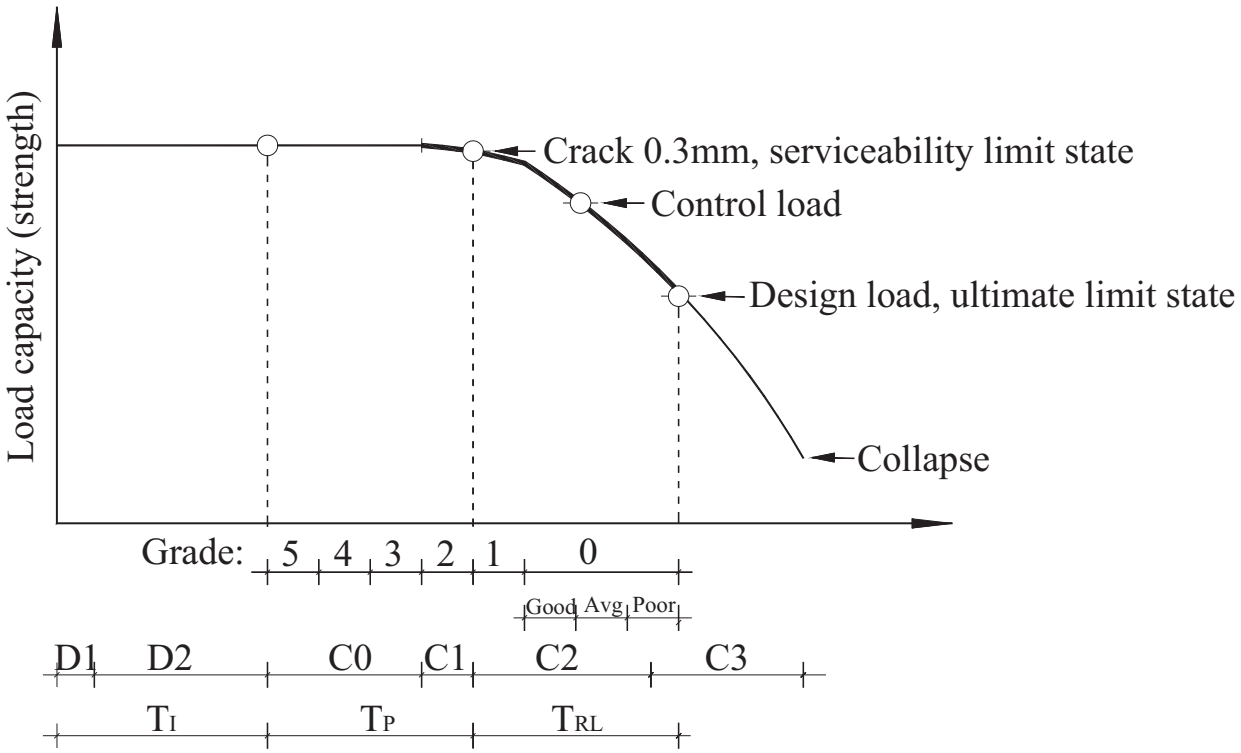

Fig. 3. Load-bearing capacity model for a RCM. Based on Torres-Acosta et al. (2007) and current study with the addition of research results by Heymsfield et al. (2007); Li et al. (2008)

As corrosion progresses, there will be an increasing build-up of corrosion products and associated increased radial stresses, causing longitudinal cracking and, eventually, concrete spalling. In this study, the unacceptable level is defined as corrosion-induced crack in longitudinal rib of a panel if it is more than 0.3mm wide (grade 1). This might also be implied as serviceability limit state of a ribbed panel. Li et al. (2008) stated that once the structure is considered to be unserviceable due to corrosion-induced cracking, there is considerable lifetime left before the structure can be considered to be unsafe. Residual life stage T_{RL} starts from the time the structure becomes unserviceable until the ultimate limit state is reached, before structural collapse.

The categorization of 'good', 'average' and 'poor' by Heymsfield et al. (2007) is also included in Fig. 3. An attempt has to be made to add the six detailed phases of the phenomenological model (Li et al., 2008) for steel corrosion in concrete. However, the model by Li et al. (2008) has a different approach. The latter differentiates six phases (D1, D2, C0, C1, C2, C3) from the mechanics of corrosion applied to the steel bar at a generic cross section of a reinforced concrete member. In addition, the initiation period of the model was based on corrosion induced by chloride attack. It was found that, for practical flexural members subject to chloride attacks, corrosion initiation may start quite early in their service life (Li et al., 2008).

As mentioned before, all panels with visual grade 1 or higher overreached the control load, which explains the location of control load on time axis. Since the structural engineering designers based their calculations on design load, the latter is employed as an equivalent of ultimate limit state in Fig. 3. Thick load capacity line in Fig. 3 represents the period for RCM covered by current structural tests. As observed in Fig. 2 and Fig. 3, the structural load capacity remains almost the same during initiation and propagation period until reaching grade 0 (in residual life period), where the capacity decrease rate is accelerated.

Investigations have been conducted during the past three decades regarding chloride or CO_2 penetration and prediction of corrosion initiation (T_I length). However, few investigators have dealt with corrosion propagation T_P and even less with residual life T_{RL} predictions, which are also needed for durability forecasting (Torres-Acosta et al., 2007). Unfortunately, structural tests with real existing structures are scarce in literature.

Since research data on the residual flexural capacity of the existing structures are rare, the results of the current study are compared to those of accelerated corrosion. However, accelerated corrosion processes simulating real structure corrosion degradation are quite complicated and do not always give comparable results (Torres-Acosta et al., 2007). Commonly, the galvanostatic method is used for accelerating steel bar corrosion in concrete. The surface characteristics of the corroded steel bar, however, are found to be different when corrosion is induced by the galvanostatic method or by the natural environment (Yuan et al., 2007).

Flexural behaviour and failure mode of existing ribbed panels. The flexural behaviour of all test panels is presented in Fig. 4-7 in terms of their load-deflection curves. The curves of panel with grade 2 or higher (no visual

deterioration or micro-cracks in longitudinal ribs) are shown with a solid line. A dashed line with long dashes or short dashes describes the load-deflection curve of panels, which received grade 1 or 0, respectively. Panels from the same test series have identical curve markers (if any). Generally, curve markers denote different load increments, except for Fig. 5, where no data has been left to describe different load increments (of panels PNS-3).

Fig. 4 shows the load-deflection curves of 14 reinforced concrete panels of mark PKZH-2. Fig. 4 presents that panels with a lower visual grade tend to have larger deflections at the same load. For example, at control load panel with grade 2 has deflected 6mm, while panels with grade 1 (except for K-5) and 0 have deflected 8…10mm and at least 17mm, respectively. Panels K-3, K-6 and K-8 (with grade 0) deflected at least 40mm at the control load. This trend conforms to Azad et al. (2007), who found that corroded beams had higher deflection than the corresponding control beams at the same load due to degrading stiffness. However, Azad et al. (2007) applied sodium chloride and direct current to initiate and accelerate corrosion, respectively, which complicates the comparison with the current study. It should be noted that only a limited amount of panels of different grades is presented in Fig. 4-7.

The statement that lower grade panels have larger deflections is not clear with panels PNS-3, PNS-12 and PNS-14 in Fig. 5-7. Yet, the majority of panels with grade 0 exhibited larger deflections under load than panels with higher grades.

Although not measured in all test panels, significant initial deflection might appear in existing panels after long-term service. The authors have found that some panels PNS-12 with visual assessment grade 0 differed from others by their relatively large initial deflections of 18mm or more and herewith failed to meet the limit state of deflection. Apart from the loss of flexural capacity, reinforcement corrosion is the primary cause of higher deflections that may lead to serviceability problems.

Of the 46 panels tested, flexural ductile mode of failure was noticed in 36 panels in Table 3. These panels reached a yield plateau, where deflections increased rapidly without considerable load addition. The unconventional failure mode of other 10 panels is marked in superscript on the panel's label in Fig. 4-7. All those 10 panels had serious visual corrosion deterioration and received either grade 0 (7 panels) or grade 1 (3 panels). However, 16 panels with visual grade 0 and 18 panels with grade 1 were tested. The one-way ANOVA did not reveal significant effect of failure mode on average grade of panel, $F(5,44) = 1.59$; $p = 0.18$.

Fig. 4 shows that panels K-1, K-7 and K-10 exhibited no yield plateau. Panels K-1, K-7 failed due to rebar fracture in transversal rib. Accumulation of sand in the middle of transversal rib might have caused that mode of failure. Longitudinal rib of panel K-10 failed near support. Concrete in failure place was crumbled prior to loading tests probably because of poor construction quality. Longitudinal rib of panel K-6 failed in mid-span region due to rebar fracture although panel demonstrated yielding (in Fig. 4) before fracture. Of the 50 panels, only panel K-6 demonstrated longitudinal rebar fracture. Corrosion caused severe reduction of cross-section in longitudinal rebar of panel K-6 was detected on visual inspection. Unfortunately no rebar tensile test was performed in test series K-1…K-7 to verify the ultimate strength or ductility of longitudinal rebar in panel K-6.

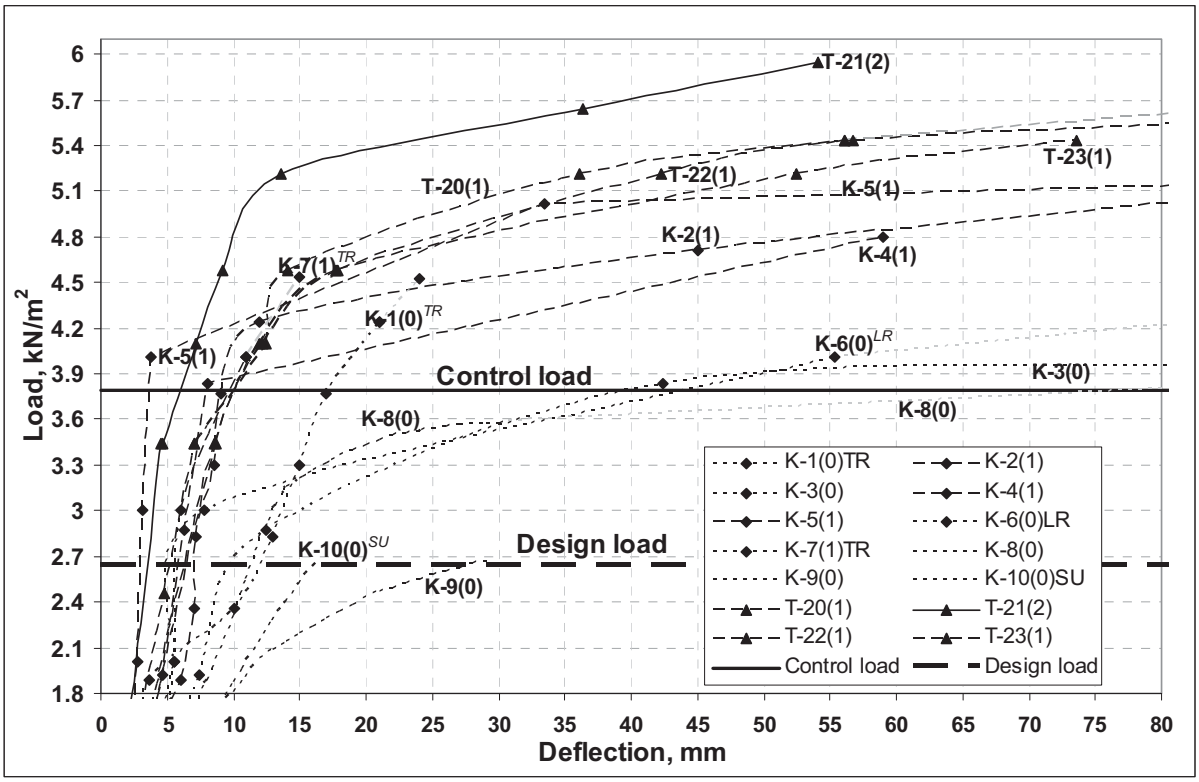

Fig. 4. Load-deflection curves of 14 reinforced concrete panels PKZH-2

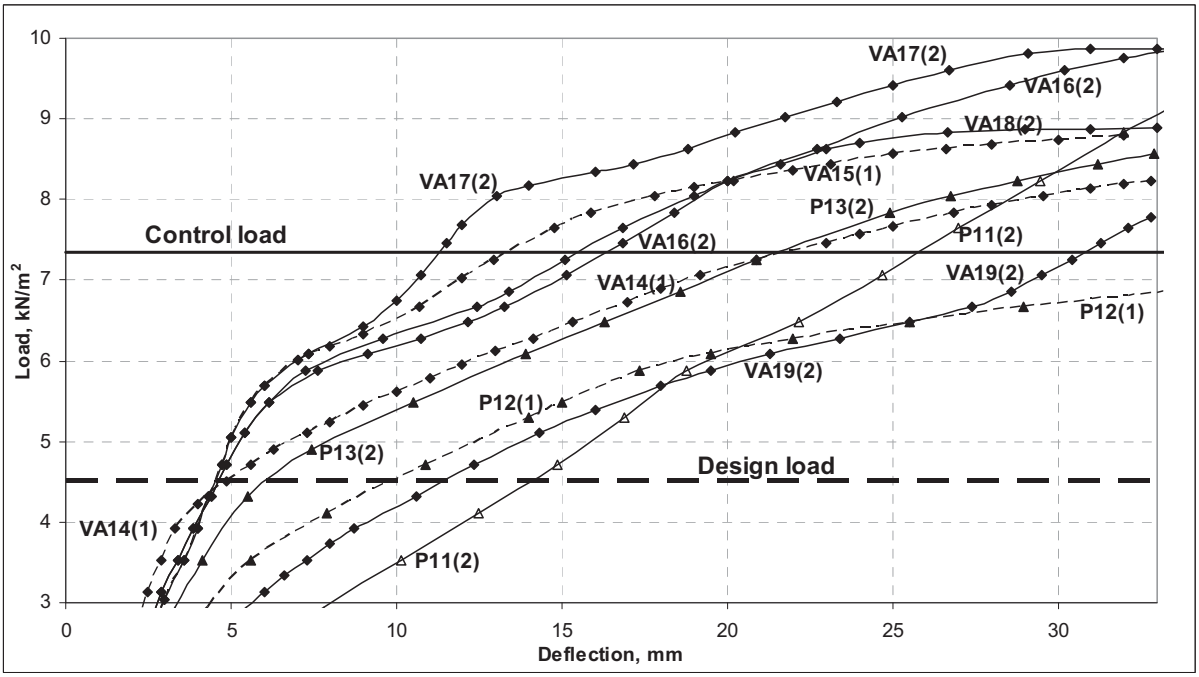

Fig. 5. Load-deflection curves of 9 prestressed concrete panels PNS-3

Fig. 4 shows that panels K-1, K-7 and K-10 exhibited no yield plateau. Panels K-1, K-7 failed due to rebar fracture in transversal rib. Accumulation of sand in the middle of transversal rib might have caused that mode of failure. Longitudinal rib of panel K-10 failed near support. Concrete in failure place was crumbled prior to loading tests probably because of poor construction quality.

Longitudinal rib of panel K-6 failed in mid-span region due to rebar fracture although panel demonstrated yielding (in Fig. 4) before fracture. Of the 50 panels, only panel K-6 demonstrated longitudinal rebar fracture. Corrosion caused severe reduction of cross-section in longitudinal rebar of panel K-6 was detected on visual inspection. Unfortunately no rebar tensile test was performed in test series K-1…K-7 to verify the ultimate strength or ductility of longitudinal rebar in panel K-6.

The failure mode of all nine panels PNS-3 was flexural ductile, which could also be deduced from the load-deflection plots in Fig. 5. The almost linear curve of panel P11 should be pointed out. The other panels PNS-3 demonstrated yielding.

Pre-stressing bars are welded to the details at the support ends of panels PNS-12 and PNS-14 (series PK-01-111, 1961). Weld rupture at support occurred with panels R7 (Fig. 6), L7 and L8 (Fig. 7). These panels showed also a relatively low (but not significant) q_u/q_c ratio when compared to other panels.

Panels V8 (in Fig. 6), L10 and V12 (in Fig. 7) failed in shear with a large inclined crack appearing at the point of concentrated load application. This type of failure can be accounted for by the four-point bending loading arrangement involved.

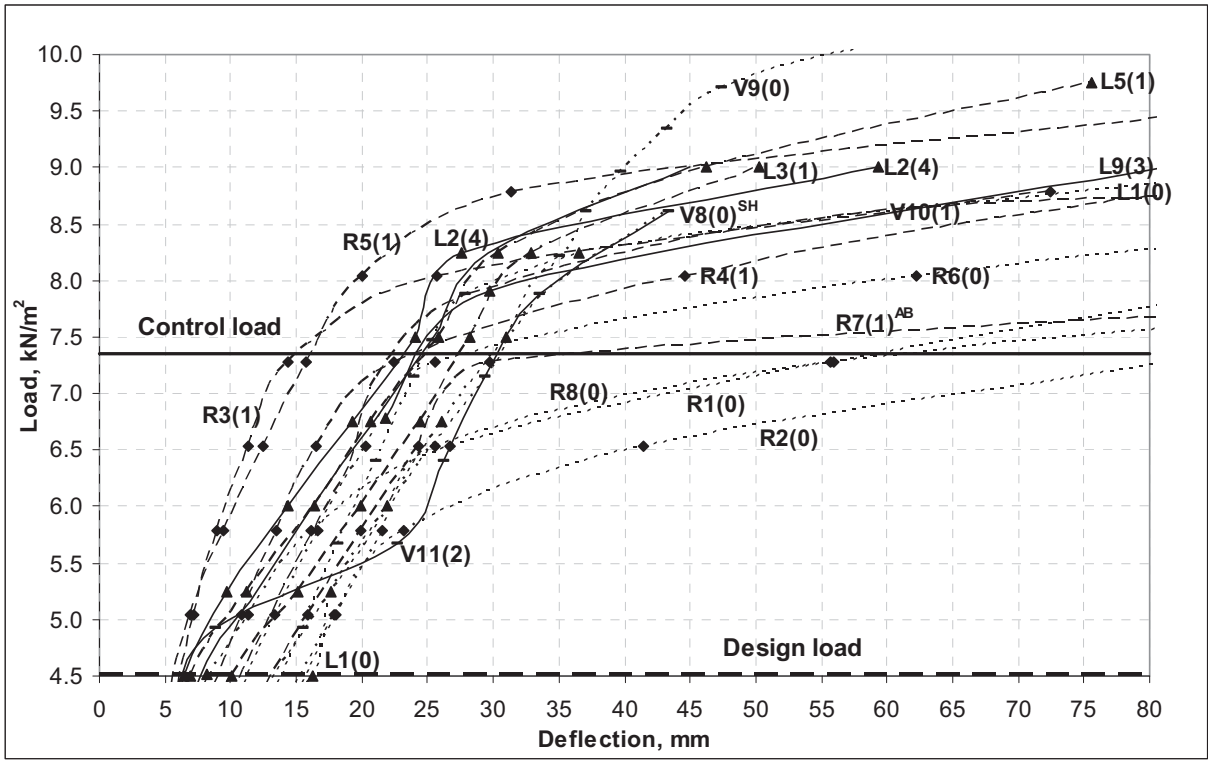

Fig. 6. Load-deflection curves of 18 prestressed concrete panels PNS-12

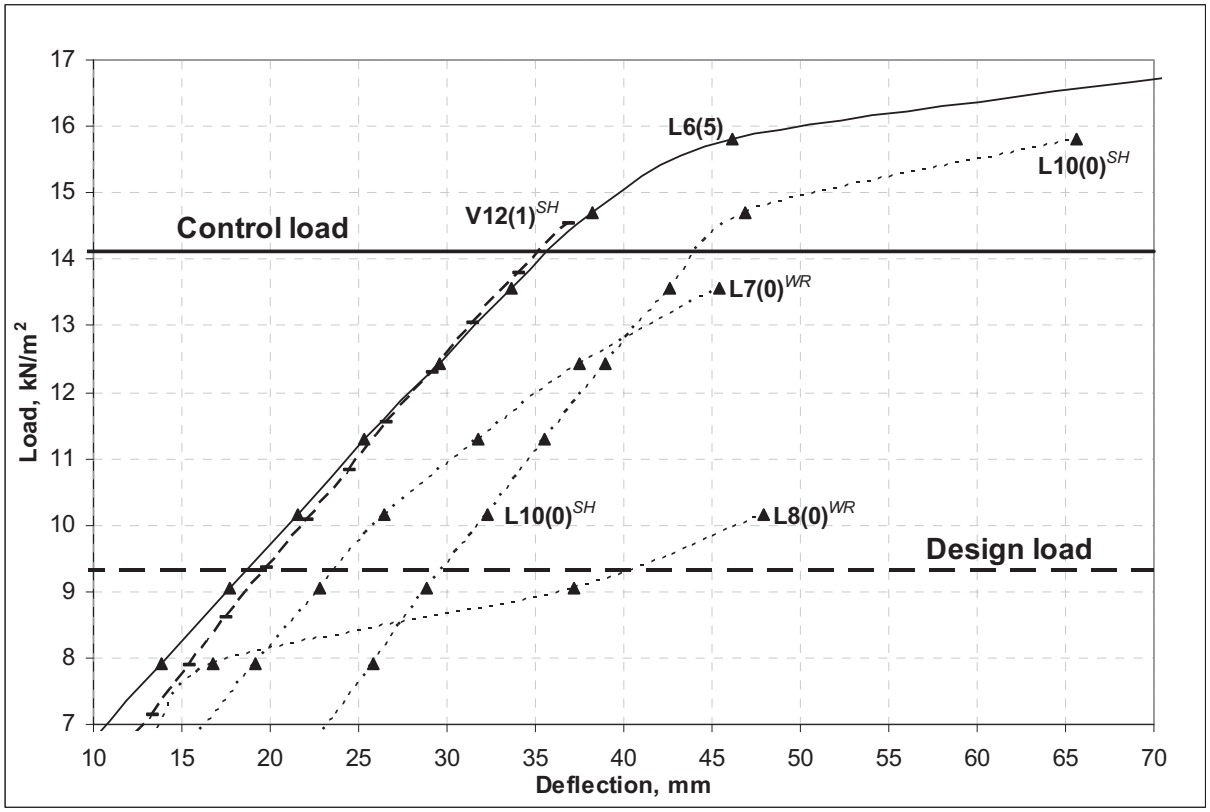

Fig. 7. Load-deflection curves of 5 prestressed concrete panels PNS-14

CONCLUSIONS

Based on the results of the current experimental investigation of the existing precast concrete ribbed panels, the following conclusions can be drawn:

1. All panels, the ultimate load of which was lower than that of the control load, received grade 0 on visual rating scale. Consequently, attention should be paid to panels where the concrete cover of longitudinal reinforcement has spalled (grade 0), which could be a sign of decreasing load capacity.
2. The majority of panels with grade 0 exhibited larger deflections under load than panels with higher grades. Apart from the loss of flexural capacity, reinforcement corrosion also produces higher deflection that may lead to serviceability problems.
3. Of the 46 panels tested, flexural ductile mode of failure was noticed in 36 panels. Other 10 panels had serious visual corrosion deterioration and received either grade 0 (7 panels) or grade 1 (3 panels).

REFERENCES

Almusallam, A.A., Al-Gahtani, A.S., Aziz A.R. & Rasheeduzzafar. 1996. Effect of reinforcement corrosion on bond strength. *Constr. & Build. Mat.* **10**(2), 123-129.

Almusallam, A.A., Al-Gahtani, A.S., Maslehuddin, M., Khan, M.M. & Aziz, A.R. 1997. Evaluation of repair materials for functional improvement of slabs and beams with corroded reinforcement. *Proc. of the Inst. of Civil Eng., Struct. and Build.* **122**, 27-34.

Azad, A.K., Ahmad, S. & Azher, S.A. 2007. Residual strength of corrosion-damaged reinforced concrete beams. *ACI Mat. J.* **104**(1), 40-47.

Durham, S.A., Heymsfield, E. & Tencleve, K.D. 2007. Cracking and reinforcement corrosion in short-span precast concrete bridges. *J. of Perf. of Constr. Facil.* **21(**5), 390-397.

GOST 7740-55. 1955. *Reinforced concrete ribbed slabs of industrial building*. Moscow, 16 pp. (in Russian).

GOST 8829-85. 1985. *Concrete and reinforced concrete prefabricated structures and products. Loading test methods and assessment of strength, rigidity and crack resistance*. Moscow, 24 pp. (in Russian).

Heymsfield, E., Durham, S.A. & Jones, J.X. 2007. Structural behaviour of short span precast channel beam bridges without shear reinforcement. *J. of Bridge Eng.* **12(**6), 794-800.

Higgins, C. & Farrow III, W.C. 2006. Tests of reinforced concrete beams with corrosion-damaged stirrups. *ACI Struct. J.* **103**(1), 133-141.

Huang, R. & Yang, C. C. 1997. Condition assessment of reinforced concrete beams relative to reinforcement corrosion. *Cem. & Concr. Comp.* **19,** 131-137.

Li, C-Q., Yang, Y. & Melchers, R.E. 2008. Prediction of reinforcement corrosion in concrete and its effects on concrete cracking and strength reduction. *ACI Mat. J.* **105**(1), 3-10.

Mangat, P.S. & Elgarf, M.S. 1999. Flexural strength of concrete beams with corroding reinforcement. *ACI Struct. J.* **96**(1), 149-158.

Miljan, J. 1977. Full scale examination of the condition of reinfored concrete structures in livestock buildings. *Transact. of Est. Agric. Acad.* 26-32. (in Estonian).

Miljan, R. 2005. *The impact of cowshed modernisation on the economic capability of milk producers in Estonia.* PhD thesis. Estonian Agricultural University, Tartu, 195 pp. (in Estonian).

Rodriguez, J., Ortega, L.M. & Casal, J. 1997. Load carrying capacity of concrete structures with corroded reinforcement. *Constr. & Build. Mat.* **11**(4), 239-248.

Series PK-01-111. 1961. *Prestressed concrete ceiling panels of dimensions 1.5 by 6m.* Construction drawings. Central institute of typical design projects, Moscow, 20 pp. (in Russian).

Tachibana, Y., Maeda, K., Kajikawa, Y. & Kawuamura, M. 1990. Mechanical behaviour of RC beams damaged by corrosion of reinforcement. In Page C.L., Treadaway, K.W.J. & Bamforth, P.B. (eds.): *Corrosion of reinforcement in concrete.*

Torres-Acosta, A., Navarro-Gutierrez, S. & Teran-Guillen, J. 2007. Residual flexure capacity of corroded reinforced concrete beams. *Eng. Struct.* **29**(6), 1145-1152.

Yuan, Y., Ji, Y. & Shah, S.P. 2007. Comparison of two accelerated corrosion techniques for concrete structures. *ACI Struct. J.* **104**(3), 344-347.